

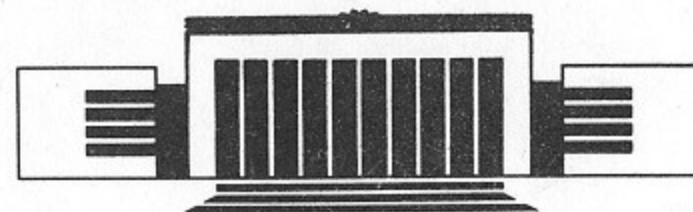


18  
ИНСТИТУТ ЯДЕРНОЙ ФИЗИКИ СО АН СССР

A.E. Blinov, V.E. Blinov, A.E. Bondar,  
A.D. Bukin, V.R. Groshev, S.G. Klimenko,  
G.M. Kolachev, A.P. Onuchin, V.S. Panin,  
I.Ya. Protopopov, A.G. Shamov, V.A. Sidorov,  
Yu.I. Skovpen, A.N. Skrinsky, V.A. Tayursky,  
V.I. Telnov, Yu.A. Tikhonov, G.M. Tumaikin,  
A.E. Undrus, A.I. Vorobiov, V.N. Zhilich

PION PAIR PRODUCTION  
IN PHOTON-PHOTON COLLISIONS

PREPRINT 91-71



НОВОСИБИРСК

## Pion pair production in photon-photon collisions.

A.E.Blinov, V.E.Blinov, A.E.Bondar, A.D.Bukin, V.R.Groshev,  
S.G.Klimenko, G.M.Kolachev, A.P.Onuchin, V.S.Panin,  
I.Ya.Protopopov, A.G.Shamov, V.A.Sidorov, Yu.I.Skovpen,  
A.N.Skrinsky, V.A.Tayursky, V.I.Telnov, Yu.A.Tikhonov,  
G.M.Tumaikin, A.E.Undrus, A.I.Vorobiov, V.N.Zhilich

### Abstract

The process  $\gamma\gamma \rightarrow \pi^+\pi^-$  has been measured with the detector MD-1 at VEPP-4. The two-photon reactions of  $e^+e^-$ ,  $\mu^+\mu^-$  and  $\pi^+\pi^-$  pair production were separated using scintillation counters, Cherenkov counters and shower-range chambers. The radiation width  $\Gamma_{\gamma\gamma}(f_2(1270)) = 3.1 \pm 0.35 \pm 0.35$  keV has been obtained.

### 1. Introduction

The process of two-photon  $\pi^+\pi^-$ -pair production was studied already in many experiments /1-9/ in the reaction

$$e^+e^- \rightarrow e^+e^- + \pi^+\pi^- \quad (1).$$

It was found that the dominant contribution to the cross section is given by  $f_2(1270)$ -meson, interfering with a non-resonant background. At small  $\pi^+\pi^-$ -masses the experiments with DM1/DM2/10/ and PLUTO/6/ observed a considerable excess in the cross section over pure Born term. Recent experiments with Mark-II on  $\gamma\gamma \rightarrow \pi^+\pi^-$ /9/ and Crystal Ball/11/ and JADE/12/ on  $\gamma\gamma \rightarrow \pi^0\pi^0$  have not confirmed this puzzle and the problem disappeared. However, even after dozen measurements many questions remain. For example, almost in all experimental works it was assumed that  $f_2(1270)$ -meson is produced in a helicity-2 state. There are some theoretical arguments for that and it follows from analyses of angular distributions (under assumption that D-wave dominates). However, it was noticed /12-14/, that the angular distribution of the helicity-2 component can be expressed as a linear combination of helicity-0 components of S and D-waves.

The analyses of the latest data show/13,14/, that solutions with large contribution of S-wave in the region above 1 GeV do not contradict the experimental data. In the present paper the latter problem is not analyzed due to poor statistics. To obtain the two-photon width of the  $f_2$ -meson we assumed, as in many other experiments, that  $f_2$ -meson is produced in a helicity-2 state and its amplitude interferes with Born term.

The important experimental problem in the analysis of the  $\pi^+\pi^-$ -final state is a large background from the two-photon reactions:

$$e^+e^- \rightarrow e^+e^- + e^+e^- \quad (2),$$

$$e^+e^- \rightarrow e^+e^- + \mu^+\mu^- \quad (3),$$

especially in the low mass region. Almost in all experiments the contributions of these reactions were calculated and subtracted (at least  $\mu^+\mu^-$ ). In this experiment the processes (1), (2), (3) are separated in the whole region above detection threshold ( $M_{\pi\pi} > 0.45 \text{ GeV}/c^2$ ).

The information on scattered electrons is not used in the present analysis.

## 2. The detector MD-1.

The experimental data were collected in 1984-1985 at the storage ring VEPP-4 with the detector MD-1. The accumulated luminosity was  $20 \text{ pb}^{-1}$  in the c.m. energy range of  $2E=7.2-10 \text{ GeV}$ . The detector and experiment has been described elsewhere/15/. Here we mention only features essential for the present analysis.

The magnetic field in the detector is transverse to the orbit plane and equals to 12 kG at the beam energy of 5 GeV. Charged particles are detected by proportional chambers. The resolution on pair masses in the process (1) equals  $\sigma_m/M=0.045+0.065 \cdot M(\text{GeV})$ .

Scintillation counters cover the coordinate system and are used for triggering, suppression of cosmic background by time-of-flight and for particle identification by  $dE/dx$ . Due to presence of material (2.5-3 cm Fe) in front of the counters they provide good electron identification.

The gaseous Cherenkov counters( $\hat{C}C$ ) are filled with ethylene at a pressure of 25 atm. and have threshold  $\gamma_{th}=5$ . In each counter Cherenkov light is detected by four photomultipliers. The average number of photoelectrons is 2.6 for  $\gamma \rightarrow \infty$  and 0.08 below threshold. In the present analysis the  $\hat{C}C$  serve for suppression of electrons.

Shower-range chambers (SRC) consist of units, containing 10 layers of proportional chambers alternating with 13 mm thick stainless steel plates. Odd planes measure X(Y)-coordinates, even- Z-coordinates. One linear output signal is taken out from each chamber for pulse height analysis. The energy resolution is

$$\sigma_E^2/E^2 = (12.6)^2 + (20.5)^2/E(\text{GeV})$$

/16/, while the angular resolution is about  $1-2^\circ$ . In the present analysis SRC are used for  $\pi/\mu$ -separation.

The luminosity was measured using processes of single bremsstrahlung and small angle Bhabha scattering. The calibration has been done using processes of double bremsstrahlung and large angle Bhabha scattering. The accuracy of the luminosity measurements is 2.5%/17/.

## 3. Event selection.

In the trigger one scintillation counter and two SRC units (or one unit, if it has hits in  $\geq 8$  planes), with hits in X(Y) and Z chambers were required.

To reject the background from bremsstrahlung and other processes with small transverse momenta a strip in SRC of  $\pm 11 \text{ cm}$  wide lying in the orbit plane was excluded from the trigger. Cosmic background was suppressed using time coincidence of scintillation counters with the beam phase.

To study the reactions (1-3) events with two oppositely-charged particle with momenta greater than  $270 \text{ MeV}/c$  were selected. Additional cut on the minimum momentum was used in order to reduce simulation time and because almost all identified  $\pi$ -mesons have larger momenta. To reject high rate background particles (mainly from single bremsstrahlung)  $P_t > 30 \text{ MeV}/c$  was required for each selected particle. The following cuts were imposed to reduce the background from cosmic rays,

$e^+e^- \rightarrow e^+e^-(\mu^+\mu^-)$  and multihadronic events:

1.  $P_i < 2500 \text{ MeV/c}$
2. acolinearity angle  $\Omega > 10^\circ$ .
3. aplanarity angle  $< 20^\circ$ .
4.  $(|P_{1t}| - |P_{2t}|) / (|P_{1t}| + |P_{2t}|) < 0.3$
5. number of scintillation counters  $\leq 3$ .
6. number of shower-range units  $\leq 2$ .

After these cuts predominantly  $e^+e^-$ ,  $\mu^+\mu^-$ ,  $\pi^+\pi^-$ -pairs of two photon nature remain in the proportion 1:2:0.4 (it follows from simulation). These ratios vary from 1:3:0.15 at  $M_{\pi\pi} = 0.5 \text{ GeV/c}^2$  to 1:2:1 at  $M_{\pi\pi} = 1.25 \text{ GeV/c}^2$  (everywhere we assign to particles the  $\pi$ -meson mass).

#### 4. Particle identification

The identification is performed in the following way. The trajectory of the particle is traced through the detector taking into account ionization losses for each possible type of the particle ( $\mu, \pi, K, p$ ). When the particle crosses any detector, the expected average parameters are calculated, i.e. ionization losses in the scintillation counter, average number of photoelectrons in the Cherenkov counter, coordinates and range (due to ionization losses only) in the shower-range chamber. This information is used for particle identification. The result obtained with M-C simulated events of the processes (1-3) are presented below. The simulation described in section 7 is a rather complete modelling of all essential processes of particle interactions in the detector.

The scintillation counters provide good identification of electrons due to  $1.7 X_0 \text{ Fe}$  in front of the counters. The pulse height distribution in the counters (reduced to normal crossing) for the processes (1) and (2) is shown in fig.1. Pulse height is measured in units of average pulse height for  $\pi$ -mesons of a given momentum. Requiring the ratio  $R = A_{SC} / \bar{A}_{SC}(\pi\text{-calc.})$  to be in the range 0.2-2.2 for each crossed counter, the number of events of the process (2) ( $e^+e^-$ -pairs) decreases by a factor of 10 at  $\epsilon_{\pi\pi} = 90\%$ , fig.2. On the contrary, to select  $e^+e^-$ -pairs it is sufficient to require  $R > 3$  for each counter and the remaining

$\pi\pi, \mu\mu$  background does not exceed 1%.

The Cherenkov counters are used in the following way. It is assumed that the particle is a  $\pi$ -meson, and the probability, that it produces photoelectrons in  $n$  photomultipliers (PM) is calculated ( $n=0,1,2,3,4$ ). If we have some triggered PM in the event, the probability  $p$  is calculated for the  $\pi$ -meson to give the same or larger numbers of PMs. The event is assigned to class, if  $p < 0.04$ . In fact, the loss of the efficiency for pions does not exceed 5%. To select  $\pi^+\pi^-$  and  $\mu^+\mu^-$ -pairs we require  $p < 0.04$  for each (at least one) particle, which crossed  $\hat{C}C$ . The residual efficiency for  $e^+e^-$ -pairs of the process (2) is plotted in fig.2. as a function of  $M_{\pi\pi}$ . In the average the  $\hat{C}C$  suppress electron pairs by a factor of 10 at  $\epsilon_{\pi\pi} = 93\%$ .

For electron rejection one additional "soft cut", based on SRC, is also used: hits in the first two chambers are required (if the particle passed farther). This gives an additional suppression of  $e^+e^-$ -pairs by a factor of 2 (see fig.2).

After applying the described cuts the process (2) has been suppressed by a factor  $\sim 250$  at 75% efficiency for  $\pi^+\pi^-$ -pairs.

The most difficult problem is  $\mu/\pi$ -separation. As was mentioned above, the  $\mu\mu/\pi\pi$  ratio equals to 20(2) at  $M_{\pi\pi} = 0.5(1.25) \text{ GeV/c}^2$ , respectively. Identification was done by ranges in the SRC. At equal momenta  $\pi$ -mesons have, as a rule, smaller ranges, than muons, due to both ionization losses and nuclear interactions. Pions are stopped in the SRC due to ionization losses up to momentum of 350-420 MeV/c, so that in  $f_2$ -meson region pions are stopped in SRC only due to nuclear interactions. For analysis we take particles, which stop inside SRC. Presented in the fig.3 is the distribution of the difference ( $\Delta R$ ) between the measured range and calculated one under assumption that it is a muon. The ranges are expressed in units of the plate thickness in the SRC (1.3cm Fe). One can see, that the  $\Delta R$ -distribution for real muons has width at half of maximum  $\sim 3$  layers and some non-gaussian tail. Besides a natural straggling, in our case a considerable contribution gives  $\Delta R$  inaccuracy of momentum measurements. The cases of large

negative values of  $\Delta R$  for muons, connected with momentum measurement errors, can be revealed partially by deviation ( $\Delta x$ ) of a measured coordinate in SRC from the calculated one. To select  $\pi^+\pi^-$ -pairs we require at least one particle with  $\Delta R < -8$  or  $\Delta R < -4$  and  $\Delta x < 50$  mm. This procedure reduces the number of  $\mu\mu$ -pairs by a factor 60 at  $\epsilon_{\pi\pi} \sim 50\%$  ( $\Delta x$ -information improves rejection twice as much). As a result of  $\mu/\pi$  separation we have obtained  $N_{\pi\pi}/N_{\mu\mu} \approx 6:1$ .

The accuracy of simulation of the nuclear interactions is not high enough, therefore the problem of systematic error arises. To make this question clear we applied the described procedure to the multihadron events both experimental and simulated. It was found that  $\pi$ -meson efficiency must be corrected by  $\approx 13 \pm 2\%$  (almost independently of the momentum). Besides the systematic error in nuclear interaction, this correction also takes into account the error due to  $\Delta x$ -cut.

#### 5. Multihadron background

Multihadron background was determined by comparison of aplanarity angle distributions in the experiment and M-C simulation. The part of multihadron events was found from the ratio of events in the range  $\Delta\phi = 10^\circ \div 20^\circ$  to all events ( $0^\circ \div 20^\circ$ ).

#### 6. Corrections.

Before comparison of the experimental data with M-C simulation the corrections have been done of all detector efficiencies.

In a part of solid angle the coordinate system of the MD-1 has the minimum number of chambers necessary for particle reconstruction, i.e. there is high sensitivity to efficiencies. The efficiencies of coordinate chambers were determined using the charged particles in the multihadron events, which have  $dE/dx$  close to that of two photon processes (with  $\mu\mu, \pi\pi$ ). To find such reference particles the hits in the SRC were used. The efficiency of the reconstruction (when there were all needed hits in chambers) was checked by events of the reaction  $ee \rightarrow \mu^+\mu^-$  which were reconstructed reliably by alternative

method using SRC information. This process was used also for determination of the accidental coincidence background. The efficiencies of SRC were measured on particles of the processes  $ee \rightarrow ee + \mu\mu(\pi\pi)$ . Spatial resolution of the coordinate chambers was determined with cosmic rays and was taken into account in the simulation.

The estimated overall systematic error of detection efficiency after corrections is  $\pm 2\%$ .

#### 7. Monte-Carlo simulation.

Two-photon processes were simulated in the equivalent photon approximation/19/.

$$d\sigma = \sigma_{\gamma\gamma}(M) dn_1 dn_2, \text{ where}$$

$$dn_i = \frac{2\alpha E E_i}{\pi q^2 \omega_i} \left( 1 - \frac{\omega_i}{E} + \frac{\omega_i^2}{2E^2} + \frac{m^2 \omega_i^2}{q^2 E^2} \right) d(-\cos(\vartheta_i)) d\omega_i$$

$$q_i^2 = \frac{m^2 \omega_i^2}{E E_i} + 2E E_i (1 - \cos(\vartheta_i)), \quad \omega_i = E - E_i, \quad M^2 = 4\omega_1 \omega_2.$$

Here:  $E$  - is the beam energy,  $E_i$  - energy of a scattered electron,  $\vartheta_i$  - the scattering angle,  $M$  - the invariant mass of a produced system. With our restrictions on  $q^2$  this formula provides percent level accuracy. Radiative corrections were not taken into account, because they do not exceed 1-2%/22/.

The cross sections of two-photon QED processes are well known and can be found elsewhere /18-21/. To increase rate of simulation the events, which a priori will not pass further cuts, were rejected before tracing through the detector (this is especially necessary for  $e^+e^- \rightarrow e^+e^-e^+e^-$ ).

The cross section of  $\gamma\gamma \rightarrow \pi^+\pi^-$  was described by Born term interfering with Breit-Wigner (B-W) amplitude of  $f_2(1270)$ -meson. It was assumed, that  $f_2$ -meson is produced in the helicity-2 state and, therefore, interferes only with Born term of the same helicity. The sign of B-W amplitude was chosen such that below  $M_f$  the interference is constructive (as it follows from previous experiments)

The B-W amplitude of  $f_2$ -meson is given by

$$T = \frac{5}{\sqrt{2s}} \frac{g \sin^2(\vartheta)}{M_f^2 - s - iM_f \Gamma}, \text{ defined so, that } \left( \frac{d\sigma}{d\Omega}(\gamma\gamma \rightarrow \pi^+\pi^-) = |T|^2 \right),$$

where  $s = M_{\pi\pi}^2$ ,

$$g(s) = M_f [\Gamma_{\gamma\gamma}^0(s) \Gamma_{\pi\pi}(s)]^{1/2} + i\Im m(g), \quad \Gamma_{\pi\pi} = 0.86 \cdot \Gamma(s),$$

$\Gamma(s)$ -full width of  $f_2$ -meson,  $\Gamma_{\gamma\gamma}^0$ -two-photon width of a direct  $f_2 \rightarrow \gamma\gamma$  transition. Imaginary part of  $g$  arises as a result of unitarization of D-wave amplitude/23,24/. Unitarization is necessary because a simple sum of Born and B-W amplitudes does not satisfy unitarity. Numerically /24/

$$\Im m g = 0.0002 \pm 0.00007 \text{ GeV}^2.$$

The two-photon width  $\Gamma_{\gamma\gamma}$  is defined by expression

$$|g|^2 = M_f^2 \Gamma_{\gamma\gamma} \Gamma_{\pi\pi}(M_f).$$

From here follows

$$\Gamma_{\gamma\gamma} = \Gamma_{\gamma\gamma}^0 + 0.257(\text{KeV}).$$

This corresponds to definition by Lyth/23/, however it is not generally accepted. The  $s$  dependence of the total width  $\Gamma(s)$  was parameterized according to/23,24/

$$\Gamma(s) = \Gamma_f \left( \frac{p}{p_0} \right)^5 \left( \frac{s_0}{s} \right)^{1/2} \left( \frac{s_0 + a}{s + a} \right),$$

where  $\Gamma_f = 0.18 \pm 0.02 \text{ GeV}$ ,  $p = 0.5 \sqrt{s - 4m_{\pi\pi}^2}$ ,  $p_0 = 0.5 \sqrt{s_0 - 4m_{\pi\pi}^2}$ ,

$$s_0 = M_f^2, \quad s = M_{\pi\pi}^2, \quad a = 0.5 \text{ GeV}^2.$$

The  $\Gamma_{\gamma\gamma}(s)$  was parameterized using the same equation with  $m_{\pi}$  replaced by  $m_{\gamma} = 0$  /24/. The cross section with such parameterization (but without unitarization) is close numerically to that used in other works/24,4,5,8 /. It should be noted that in publications on  $\gamma\gamma \rightarrow \pi^+\pi^-$ ,  $K^+K^-$  there is no agreement on a power of  $s$  in the B-W formula. Moreover, there is no generally accepted  $\Gamma_{\gamma\gamma}(s)$  dependence. Due to variety of opinions we included in our result the systematic error, corresponding to change of power by  $\pm 1$ .

The passage of particles through the detector was simulated using code UNIMOD/25/. Simulation accuracy of nuclear interaction is not sufficient, therefore, the efficiency of

$\pi$ -meson separation was corrected as it was described in the previous section. The statistics of the simulation corresponds to the integrated luminosity of  $54 \text{ pb}^{-1}$  for  $\pi^+\pi^-$ ,  $38 \text{ pb}^{-1}$  for  $\mu^+\mu^-$  and  $8 \text{ pb}^{-1}$  for  $e^+e^-$ .

## 8. Results.

### 8.1 $\gamma\gamma \rightarrow e^+e^-$

To select  $\gamma\gamma \rightarrow e^+e^-$  only one cut was imposed besides the common requirements (sect.3): the pulse height in each scintillation counter must exceed the calculated one for  $\pi$ -meson by at least a factor 3.5 (fig.4). The mass pair distribution for selected events is presented in fig.4 ( $\pi$ -meson mass is assigned to all particles) together with the the expected spectrum for  $\gamma\gamma \rightarrow e^+e^-$ . The distributions are in a good agreement ( $P(\chi^2) = 10\%$ ). The calculated fraction of  $\mu^+\mu^-$  and  $\pi^+\pi^-$  passed these cuts is less than 1 %. The  $\gamma\gamma \rightarrow e^+e^-$  process was analyzed to check the simulation of  $e^+e^-$ -pairs and to demonstrate the identification possibilities. The main verification of detector performance is based on analysis of  $\mu^+\mu^-$ -pairs.

### 8.2 $\gamma\gamma \rightarrow \mu^+\mu^- + \pi^+\pi^-$

To suppress electrons we used selection criteria based on CC,  $\hat{C}C$  and SRC, which were explained in sect.4. As a result the number of electrons was reduced by a factor of ~250 at 70-75% efficiency for  $\pi^+\pi^-$  and  $\mu^+\mu^-$ . The resulting pair mass distribution is shown in fig.5.

From these experimental data a small contribution (~2%) from processes other than  $\gamma\gamma \rightarrow \pi^+\pi^-, \mu^+\mu^-$  was subtracted. The multihadronic background was determined for each mass interval by comparison of aplanarity angle distributions in the experiment and simulation (sect.5). The  $\Delta\phi$ -distribution for all selected events is shown in fig 6. The discrepancy at small  $\Delta\phi$  can be explained by instability in beam position during the experiment. For the region  $\Delta\phi = 10-20^\circ$ , which was used for background estimation, this gives a small effect. The multihadronic background found in this way is about 1.5%.

Background from the processes with narrow  $\Delta\phi$ -distributions was found by modelling and equals:  $\gamma\gamma \rightarrow K^+K^- - 0.3\%$ ,

$\gamma\gamma \rightarrow e^+e^-$ -0.15%,  $ee \rightarrow \mu^+\mu^-$ -0.15%,  $ee \rightarrow \tau^+\tau^-$ <0.15%. Cosmic rays background was determined from the time difference distribution between scintillation counters and beam phase and accounts for less than 0.5%. Contribution of the Bhabha scattering, as follows from pulse height distribution in the shower-range chambers, is negligible also. Polar angle and collinearity angle distributions show good agreement between experiment and simulation as well..

The ratio  $N_{\text{exp}}/N_{\text{M-C}}(\mu\mu+\pi\pi)$  for the obtained data equals to  $1.015 \pm 0.016 \pm 0.03$ . The systematic error is connected with uncertainty in the expected number of  $\pi^+\pi^-$  (in the simulation  $\Gamma_{\gamma\gamma}(f_2(1270))=3$  KeV was assumed). In fact, these results confirm our understanding of the detector, precision of corrections, luminosity measurements and correctness of M-C simulation.

### 8.3 $\gamma\gamma \rightarrow \pi^+\pi^-$

As it was shown in the previous section, after electron suppression only  $\mu^+\mu^-$  and  $\pi^+\pi^-$  pairs remain in a ratio ~ 5 to 1 in average and about (15-20) to 1 in the 500-600 MeV/c<sup>2</sup> energy region, see fig.5. Muon/pion separation was done by ranges in the shower-range chambers using algorithm described in section 4. The distribution on invariant mass of pairs after pion selection is presented in fig.7, where contributions of background processes are also shown.

Multihadron background was found, as before, by comparison of aplanarity angle distributions in the experiment and M-C simulation for a each mass bin. Summary  $\Delta\phi$ -distribution is shown in fig. 8. The excess of experimental events is clearly seen at large angles. The contributions of the processes  $\gamma\gamma \rightarrow e^+e^-$ ,  $\mu^+\mu^-$ ,  $K^+K^-$  were obtained by M-C simulation. The  $\gamma\gamma \rightarrow K^+K^-$  cross section was taken from the work/25/.

The mass spectrum of  $\pi$ -pairs after background subtraction is plotted in fig.9. The data are fitted according to unitarized model of Lyth, considering Born amplitude interfering with  $f_2(1270)$ -meson (sect.7). Solid histogram is the optimum fit with the only free parameter  $\Gamma_{\gamma\gamma}(f_2)$ . The  $f_2$ -meson peak is strongly widened due to detector resolution. Histograms for different  $\Gamma_{\gamma\gamma}$  were obtained from one set of simulated events (at  $\Gamma_{\gamma\gamma} = 3$  keV)

by changing the weight of each event according to dependence of the differential cross sections on  $\Gamma_{\gamma\gamma}$ . The optimum two-photon width is

$$\Gamma_{\gamma\gamma}(f_2) = 3.1 \pm 0.35 \pm 0.35 \text{ keV.}$$

All histogram channels were included in the fit. The result changes negligibly when only  $f_2$ -meson region is taken. The systematic error is determined mainly by the following factors (in % to  $\Gamma_{\gamma\gamma}$ ): the luminosity-3.5%,  $\epsilon_{\pi\pi}$ -3.5%, multihadronic background-6%, uncertainty in parameterization of  $\Gamma(s)$  ( $\pm 1$  power of  $M_{\pi\pi}$ )-6%;  $\mu^+\mu^-$ -background -3.5%, unitary corrections-6%.

The fit without unitarization gives  $\Gamma_{\gamma\gamma}(f_2) = 2.6 \pm 0.35 \pm 0.3$  keV. Unitarization increases direct coupling width  $\Gamma_{\gamma\gamma}^0$  introduced in section 7 by 0.25 keV. Our final result contains also an additional supplement of 0.257 keV arising in the model of Lyth.

World average value  $\Gamma_{\gamma\gamma}(f_2) = 2.76 \pm 0.14$  keV/26/. The averaged experiments used various parameterizations, mostly without unitarization and none of them used Lyth's model. The latest Mark-II analysis /9,13/ gives  $\Gamma_{\gamma\gamma}(f) = 3.15 \pm 0.04 \pm 0.28$  with parameterization of Lyth. With the given comments our two-photon width is in agreement with previous results.

### Conclusion

The reactions  $\gamma\gamma \rightarrow e^+e^-$ ,  $\mu^+\mu^-$ ,  $\pi^+\pi^-$  have been studied with the detector MD-1. Good identification capabilities enabled us to separate these processes. The measured  $\gamma\gamma \rightarrow e^+e^-$ ,  $\mu^+\mu^-$  cross sections agree with QED calculations. The  $\gamma\gamma \rightarrow \pi^+\pi^-$  cross section in the region 0.45-1.6 GeV/c<sup>2</sup> agrees within the error limits with the model taking into account Born term and  $f_2(1270)$ -meson only. The radiative width  $\Gamma_{\gamma\gamma}(f_2(1270)) = 3.1 \pm 0.35 \pm 0.35$  keV has been obtained for unitarized model of Lyth.

The authors express their sincere gratitude to VEPP-4 staff for help in the work and to N.N.Achasov, V.S.Fadin, E.A.Kuraev, G.N.Schestakov and V.V.Serebryakov for consultation on theoretical questions.

References.

1. Ch. Berger et al., (PLUTO), Phys. Lett. 94B(1980) 254
2. A. Roussarie et al. (Mark 2, SPEAR), Phys. Lett. 105B(1981) 304
3. R. Brandelik et al. (TASSO), Z. Phys. C10(1981) 117
4. J. R. Smith et al., (Mark 2, PEP), Phys. Rev. D30(1984) 851
5. A. Courau et al., (DELCO), Phys. Lett. 147B(1984) 227
6. Ch. Berger et al., (PLUTO), Z. Phys. C26(1984) 199
7. H. J. Behrend et al. (CELLO), Z. Phys. C23(1984) 223
8. H. Aihara et al (PEP4/9, TPC), Phys. Rev. Lett. 57(1987) 404
9. J. Boyer et al, (Mark-2), SLAC-PUB-4595(1987)
10. Z. Ajaltonni et al., (DM1, DM2), Phys. Lett. 194(1987) 573
11. H. Marsiske et al., (Crystal Ball), Phys. Lett. D41(1990) 3324
12. T. Oest et al, (JADE), Z. Phys. C47(1990) 343
13. D. Morgan, M. R. Pennington, Z. Phys. C48(1990) 623
14. M. Feindt, J. Harjes, DESY 90-146(1990)
15. S. E. Baru et al., Z. Phys. C30(1986), 42(1989) 505, 49(1991) 239
16. A. I. Vorobiev et al., Prepr. INP 90-84, Novosibirsk 1990.
17. A. E. Blinov et al., Nucl. Instr. and Meth. A273(1988) 31
18. H. Terazawa, Rev. Mod. Phys. 45(1973) 615
19. V. M. Budnev, I. F. Ginzburg, G. L. Kotkin, V. G. Serbo,  
Phys. Rep. 15(1975) 181
20. H. Kolanoski, Two Photon Physics at Storage Rings, Springer  
Verlag, Berlin, 1984.
21. M. Poppe, Int. Journal of Modern Phys., A 1(1986) 545
22. M. Landro, K. Mork and H. Olsen, Phys. Rev. D36(1987) 44
23. D. H. Lyth, J. Phys. G 10(1984) 39, 11(1985) 459
24. R. Jonson, SLAC-Report-294, 1986. Ph. Dissertation
25. A. D. Bukin et al., Prepr. INF 84-33, Novosibirsk 1984
26. H. Albrecht et al., Z. Phys. C 48(1990) 183
27. Particle Data Group, Phys. Lett. B239(1990)

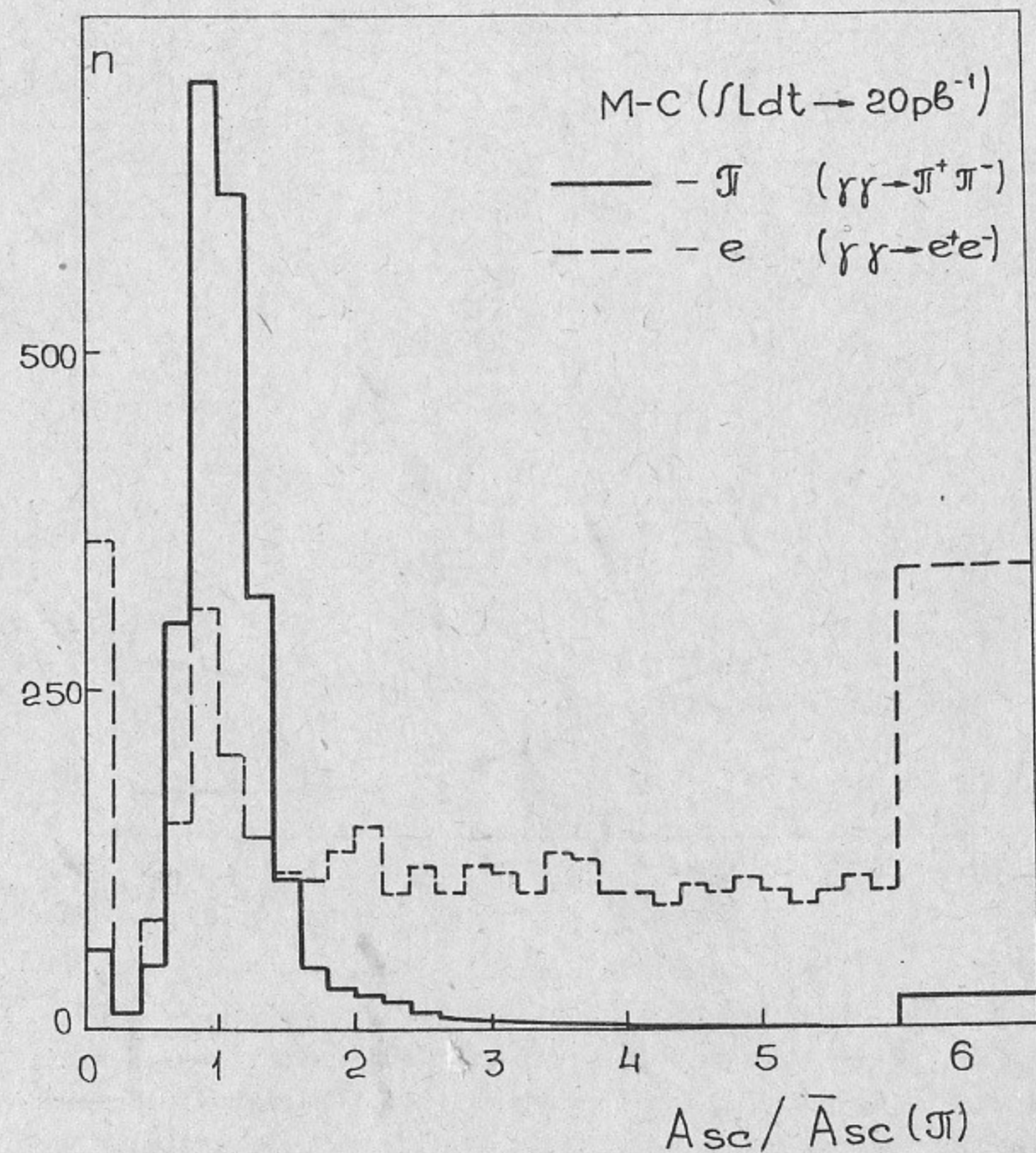


Fig. 1. Pulse height distributions in scintillation counters for the processes  $\gamma\gamma \rightarrow e^+e^-$  and  $\gamma\gamma \rightarrow \pi^+\pi^-$  (M-C-simulation).



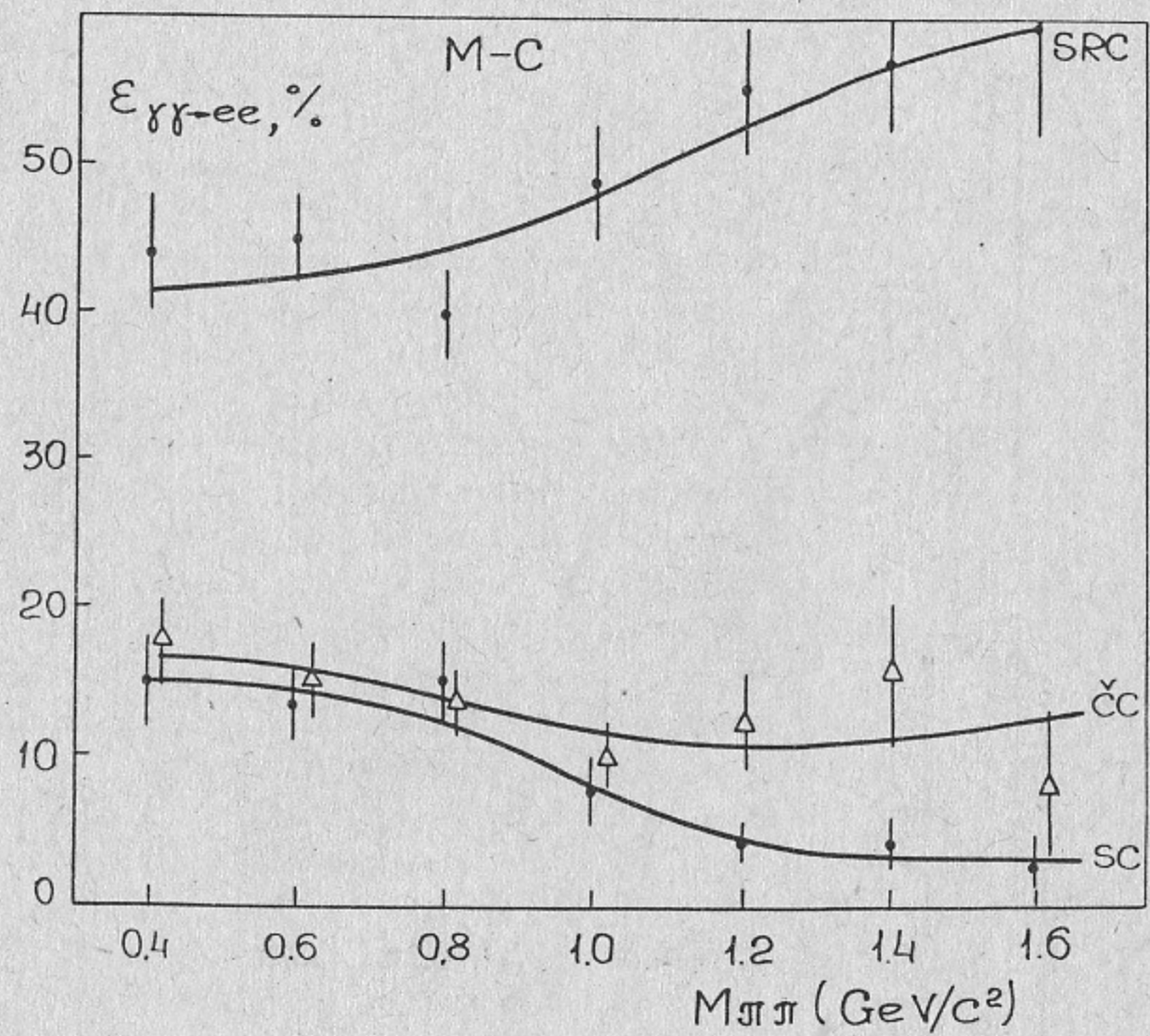


Fig. 2. Efficiency for the processes  $\gamma\gamma \rightarrow e^+e^-$  after suppression of electrons by scintillation counters (SC), Cherenkov counters ( $\hat{C}C$ ) and shower-range chambers (SRC) ("soft cut", see text).

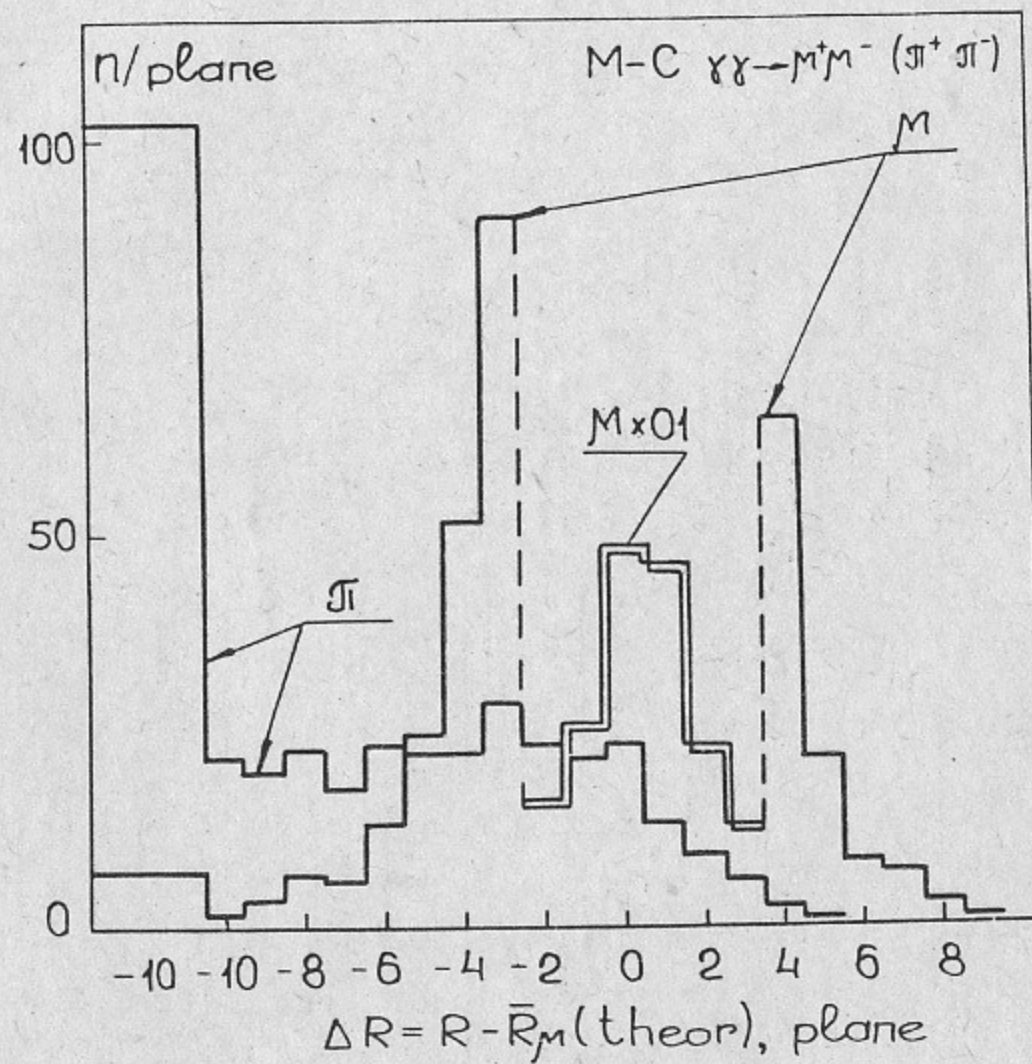


Fig. 3. The distribution in the difference between the measured range in the SRC and the calculated one (under assumption that it is muon) for particles of the processes  $\gamma\gamma \rightarrow \mu^+\mu^-$ ,  $\gamma\gamma \rightarrow \pi^+\pi^-$ .

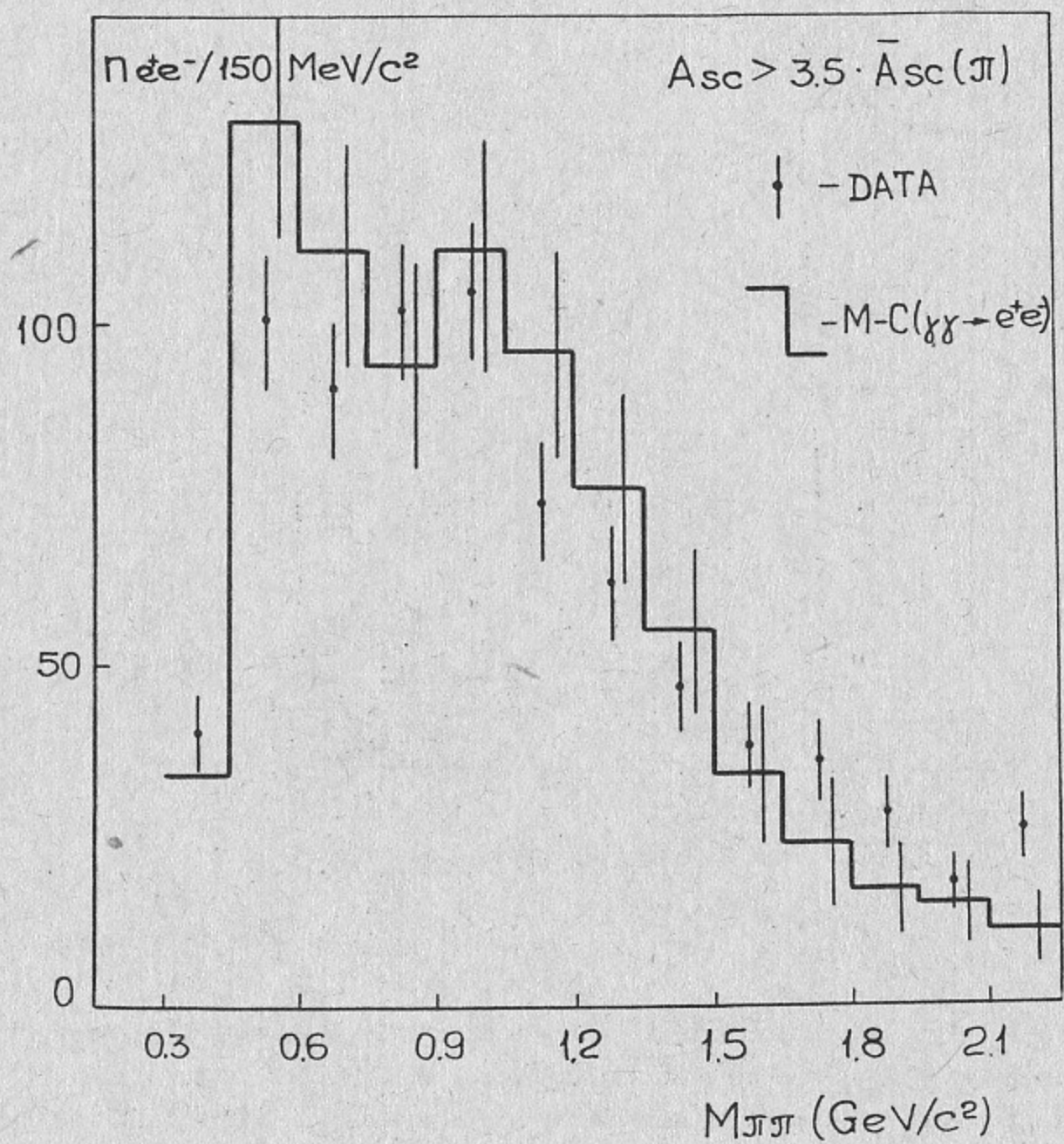


Fig. 4. The invariant mass spectrum of pairs when pulse heights in both scintillation counters  $A_1 > 3A_\pi(\text{calc.})$  are required.

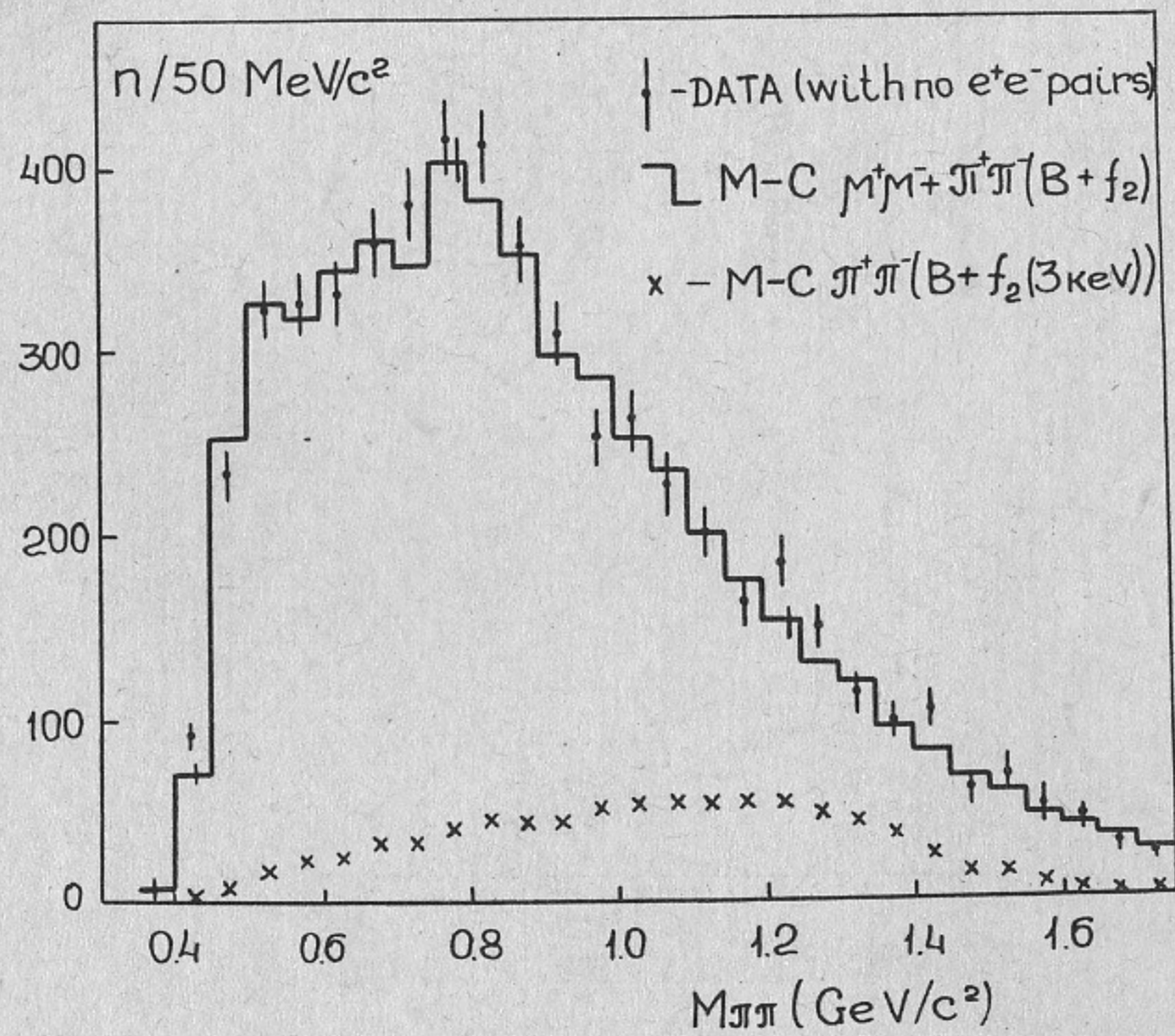


Fig. 5. The invariant mass spectrum of pairs after rejection of electrons.

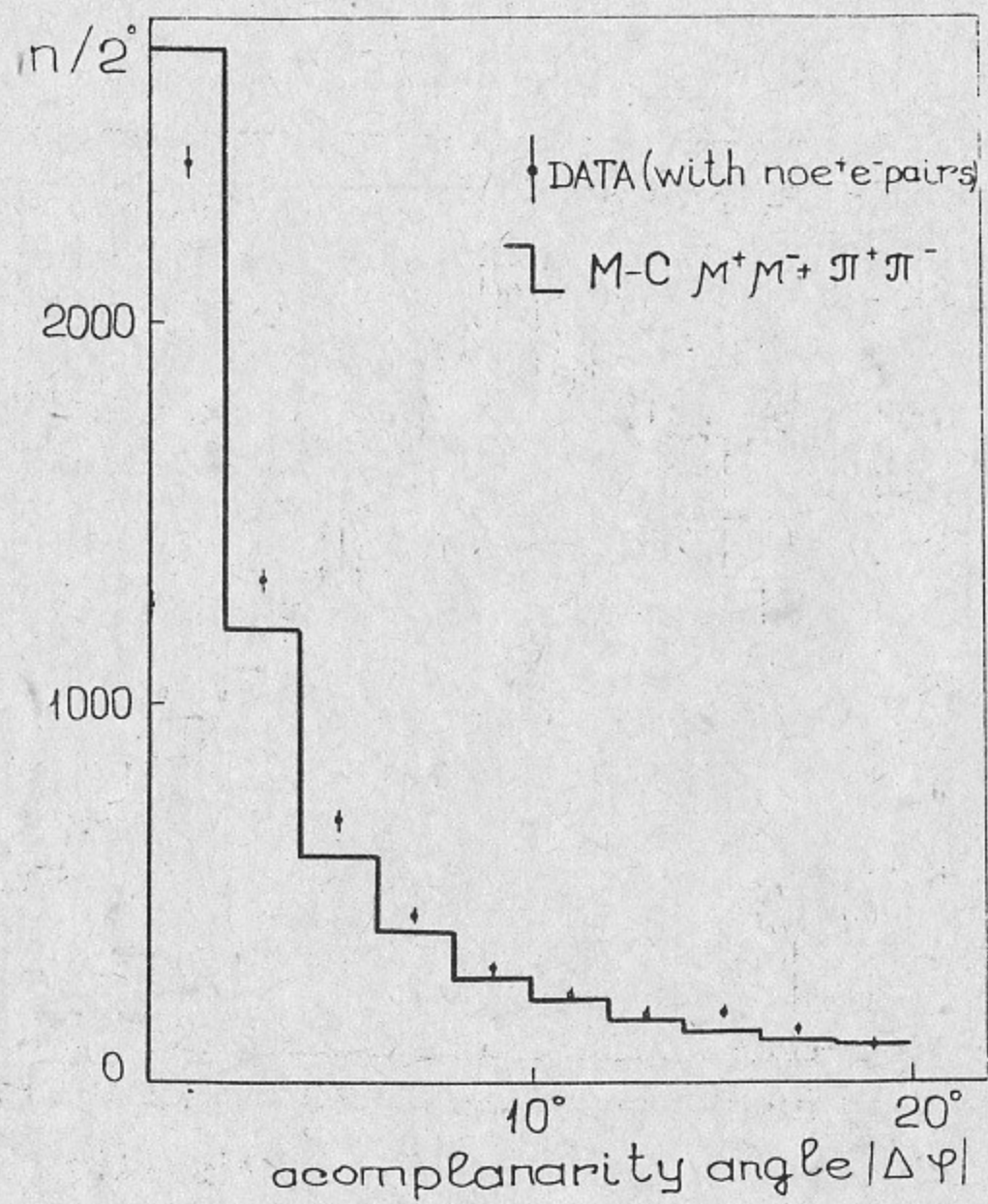


Fig. 6. Acomplanarity angle distribution after imposing kinematical cuts and rejection of electrons.

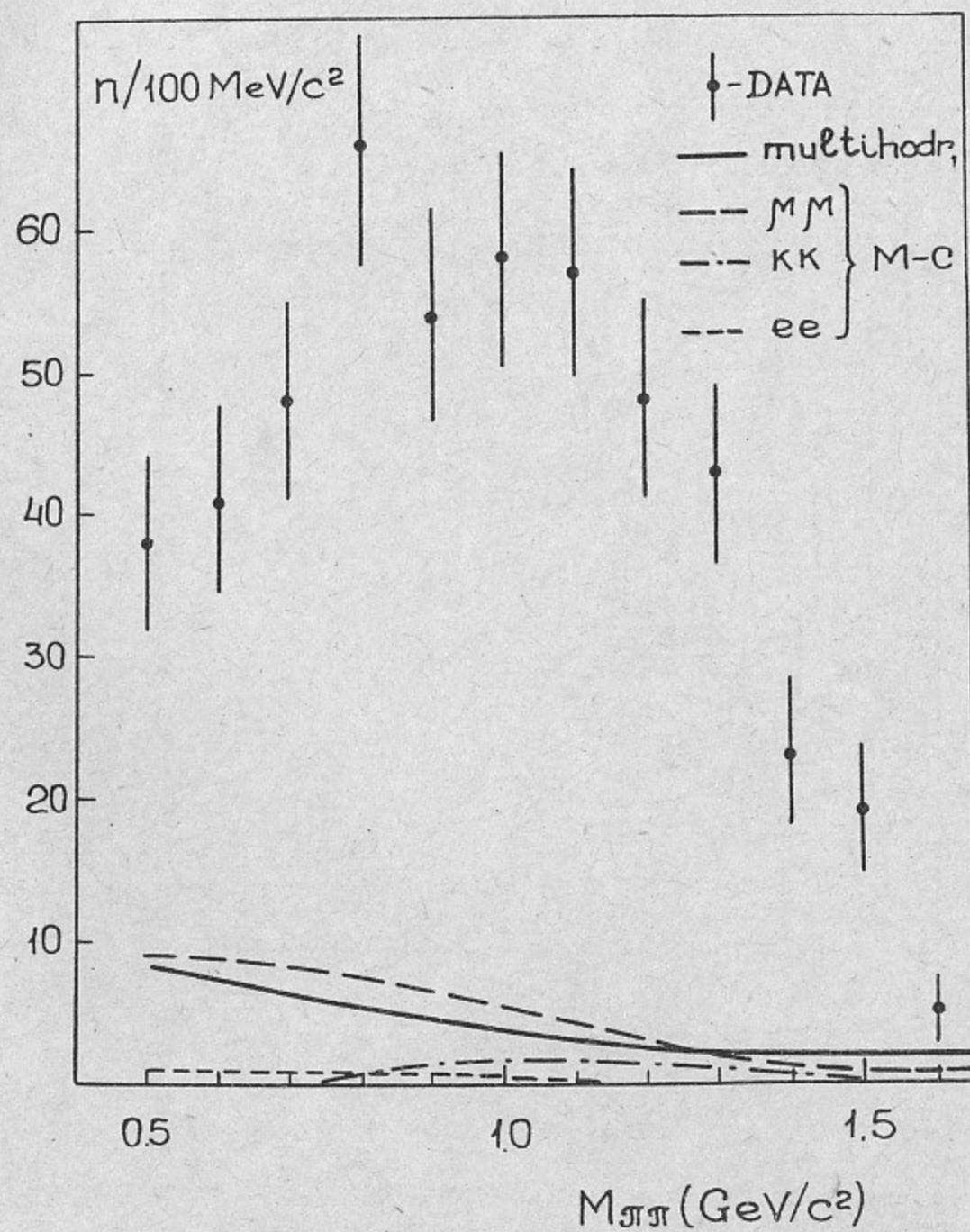


Fig. 7. The invariant mass spectrum of pairs passed the selection criteria for  $\gamma\gamma \rightarrow \pi^+\pi^-$ .

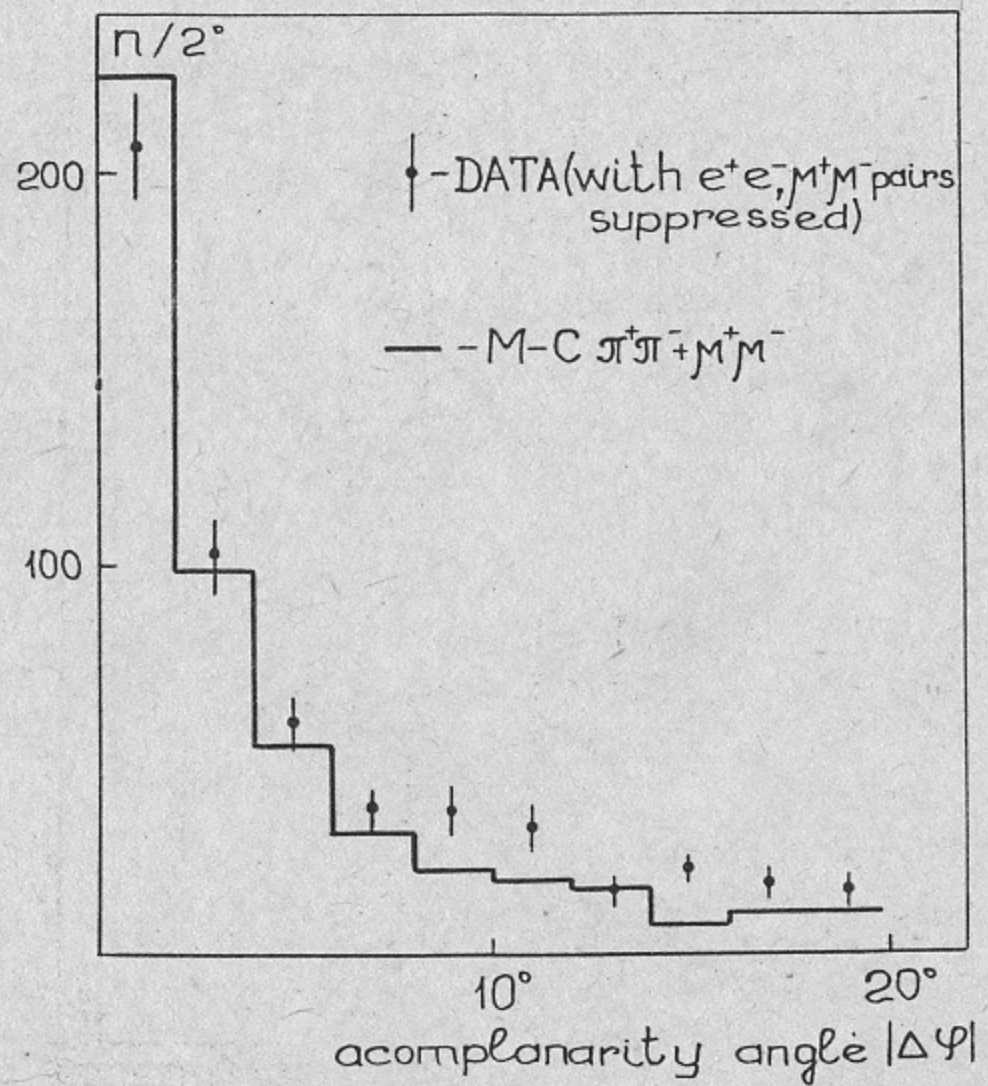


Fig. 8. Acomplanarity angle distribution for events passed the selection criteria for the processes  $\gamma\gamma \rightarrow \pi^+\pi^-$ .

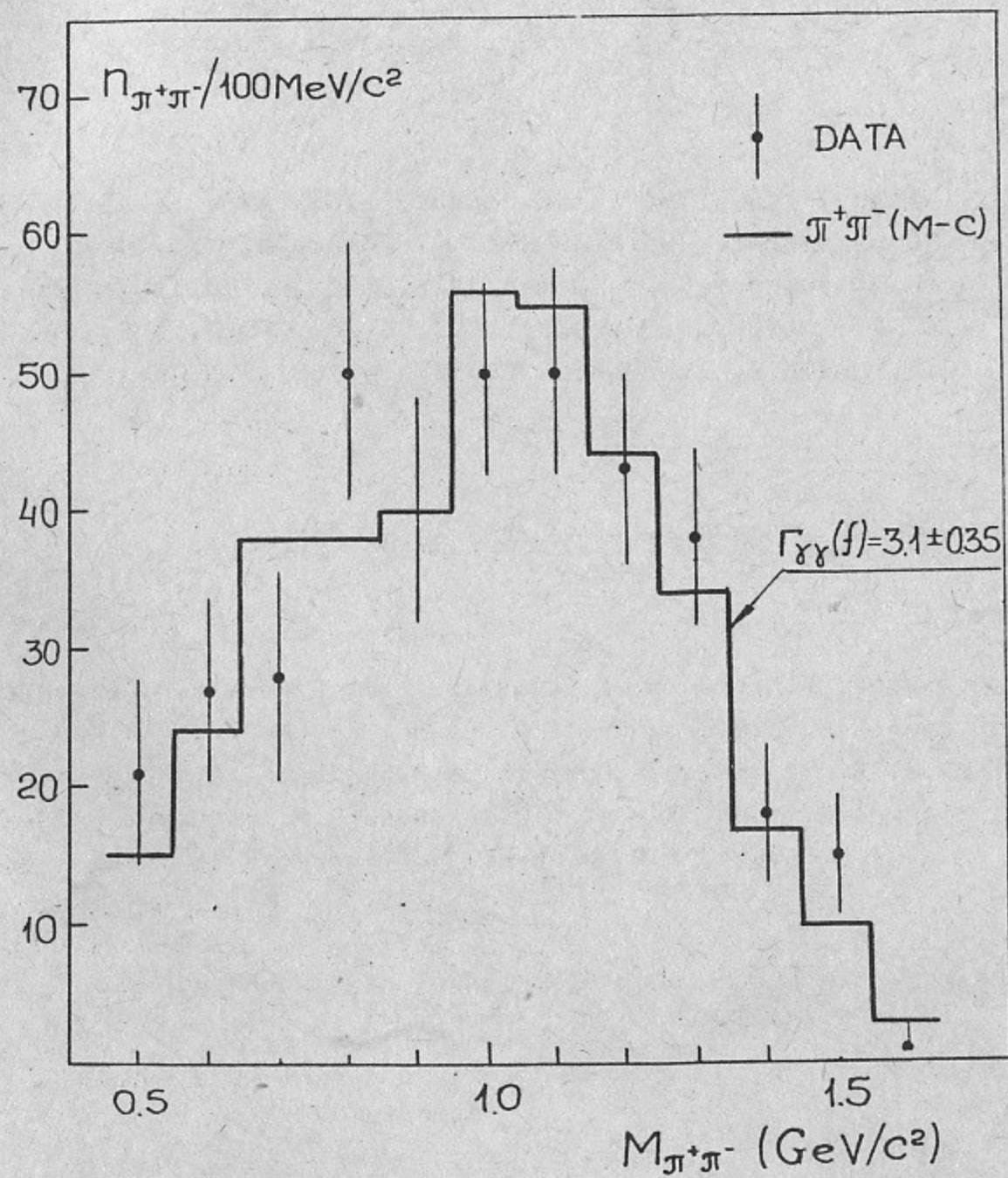


Fig. 9. The invariant mass spectrum of  $\pi^+\pi^-$ -pairs together with the optimum fit..

A.E.Blinov, V.E.Blinov, A.E.Bondar, A.D.Bukin, V.R.Groshev,  
S.G.Klimenko, G.M.Kolachev, A.P.Onuchin, V.S.Panin,  
I.Ya.Protopopov, A.G.Shamov, V.A.Sidorov, Yu.I.Skovpen,  
A.N.Skrinsky, V.A.Tayursky, V.I.Telnov, Yu.A.Tikhonov,  
G.M.Tumaikin, A.E.Undrus, A.I.Vorobiov, V.N.Zhilich

PION PAIR PRODUCTION IN PHOTON-PHOTON COLLISIONS

А.Е.Блинов, В.Е.Блинов, А.Е.Бондарь, А.Д.Букин, В.Р.Грошев,  
С.Г.Клименко, Г.М.Колачев, А.П.Онучин, В.С.Панин, И.Я.Про-  
топов, А.Г.Шамов, В.А.Сидоров, Ю.И.Сковпень, А.Н.Скринский,  
В.А.Таярский, В.И.Тельнов, Ю.А.Тихонов, Г.М.Тумайкин,  
А.Е.Ундрус, А.И.Воробьев, В.Н.Жилич

РОЖДЕНИЕ ПАР ПИОНОВ В ФОТОН-ФОТОННЫХ СТОЛКНОВЕНИЯХ

Препринт 91-71

Работа поступила 10 июля 1991 года

Ответственный за выпуск С.Г.Попов

Подписано к печати 15 июля 1991 года

Формат бумаги 60x90 1/16. Объем 1,5 печ.л., 1,2 уч.-изд.л.

Тираж 220 экз. Бесплатно. Заказ № 71

---

Ротапринт ИЯФ СО АН СССР, г.Новосибирск, 90.